The Company of Biologists

SHORT COMMUNICATION

Photoreceptor signalling is sufficient to explain the detectability threshold of insect aerial pursuers

Elisa Rigosi[1,*], Steven D. Wiederman[2] and David C. O'Carroll[1]

ABSTRACT

An essential biological task for many flying insects is the detection of small, moving targets, such as when pursuing prey or conspecifics. Neural pathways underlying such 'target-detecting' behaviours have been investigated for their sensitivity and tuning properties (size, velocity). However, which stage of neuronal processing limits target detection is not yet known. Here, we investigated several skilled, aerial pursuers (males of four insect species), measuring the target-detection limit (signal-to-noise ratio) of light-adapted photoreceptors. We recorded intracellular responses to moving targets of varying size, extended well below the nominal resolution of single ommatidia. We found that the signal detection limit (2× photoreceptor noise) matches physiological or behavioural target-detection thresholds observed in each species. Thus, across a diverse range of flying insects, individual photoreceptor responses to changes in light intensity establish the sensitivity of the feature detection pathway, indicating later stages of processing are dedicated to feature tuning, tracking and selection.

KEY WORDS: Target detection, Vision, Contrast sensitivity, Retina, Signal-to-noise ratio, Feature detection

INTRODUCTION

Visual systems optimized to detect moving targets are common across the animal kingdom (Nordström and O'Carroll, 2009; Sanes and Zipursky, 2010). For example, some insects have eye subregions with higher optical acuity associated with dedicated neuronal pathways for discrimination of small moving targets, even those embedded within cluttered visual surrounds (Nordström and O'Carroll, 2009; Hardie, 1985; Strausfeld, 1991). In diverse species, identified small target motion detector (STMD) neurons in the third optic ganglia are tuned to target size and velocity, and are sensitive to target contrast (Nordström and O'Carroll, 2009; Collett, 1971; O'Carroll, 1993; Nordström et al., 2006; Trischler et al., 2007).

In addition to electrophysiology, behavioural observations have established target-pursuit capabilities of flying insects. A previous body of literature has shown that insect target-detection pathways frequently respond to targets considerably smaller than the sampling resolution of the eye (O'Carroll, 1993; O'Carroll and Wiederman, 2014; Nordström et al., 2006; Vallet and Coles, 1993; Wardill et al., 2015; Somanathan et al., 2017). If presented with a slowly moving

[1]Department of Biology, Lund University, Sölvegatan 35, S-22362 Lund, Sweden. [2]Adelaide Medical School, The University of Adelaide, Adelaide, SA 5005, Australia.

*Author for correspondence (elisa.rigosi@biol.lu.se)

E.R., 0000-0002-2283-1257

target, the strength of photoreceptor responses predominantly reflects the interaction between the target's angular size and the photoreceptor receptive field (i.e. the neural image; O'Carroll and Wiederman, 2014). Smaller targets induce smaller increments (light targets) or decrements (dark targets) in the number of photons captured. At threshold, responses elicited by a tiny target will be indistinguishable from noise induced by the stochastic nature of light (photon shot noise) or variability in the signal generated by transduced photons (Lillywhite, 1977; Laughlin and Lillywhite, 1982). Target detection thus depends not only on angular resolution but also on photon catch and thus on the visual ecology of the animal (Land, 1997).

Whilst insect optics and retinal processing inherently contribute to target-detection limits, additional non-linear processing within neural pathways for target detection could potentially boost very weak signals buried below the noise of single receptors (Burton and Laughlin, 2003). Dragonfly STMD neurons, for example, show profound facilitation for targets moving along long, continuous paths, suggesting that feed-forward mechanisms amplify features that otherwise fall below noise thresholds (Nordström et al., 2011; Wiederman et al., 2017). However, direct quantitative comparisons between the limits of higher-order target detection and those imposed by retinal sampling are scarce. Here, we compared the sampling strategies utilized by four insect groups, whose target-tracking performance has been studied either behaviourally or electrophysiologically. Is the limit of higher-order target detection determined by this photoreceptor constraint or does the downstream neuronal architecture implement a clever signal-extraction algorithm? By measuring photoreceptor responses (target signal and photoreceptor noise) in response to small targets moved across a bright LCD display, we found that photoreceptors impose the constraint. Across all four species investigated, detection thresholds were remarkably well matched to the known behavioural and electrophysiological limits as previously described.

MATERIALS AND METHODS

Animals

Dragonflies [*Hemicordulia tau* (Selys 1871)] and hoverflies [*Eristalis tenax* (Linnaeus 1758)] were collected in the Adelaide Botanical Garden. Honey bee drones (*Apis mellifera* Linnaeus 1758) were collected at the entrance of hives in the city of Adelaide. Blowflies [*Calliphora stygia* (Fabricius 1781)] were reared from purchased larvae. Emergent adults were fed *ad libitum* with a sugar, milk powder and yeast mixture (1:1:0.25) and maintained at room temperature (24°C). Only adult males were used in this study; all dragonflies and hoverflies were netted from the wild during normal foraging behaviour. Drone bees were collected from the hive entrance. For lab-raised *Calliphora*, we used individuals aged 10–30 days. We cannot precisely specify the age of wild-caught individuals, although we avoided both freshly emerged adults (<2 days; easily recognized by weak flight and by the very soft

cuticle) and very old individuals (based on the condition of the wings, which become damaged with age).

Animal preparation and intracellular recordings

Insects were immobilized in a 1:1 wax:rosin mixture and placed in front of a flicker-free LCD monitor with rapid pixel kinetics (EIZO Foris FG2421; 1920×1080 pixels; 300 cd m^{-2}). Photoreceptors were recorded intracellularly using aluminosilicate glass capillaries (SM100F-10, Harvard Apparatus, Holliston, MA, USA) pulled in a Sutter Instruments P-97 (Novato, CA, USA) and filled with 2 mol l^{-1} KCl solution (electrode resistance 70–200 MΩ). We made small holes in the cornea to allow access to photoreceptors in the acute or bright zone of the eyes of each species. Male honey bees and hoverflies have an acute zone in the dorso-frontal part of the eye (Seidl, 1982; Menzel et al., 1991; Straw et al., 2006); in blowflies, the acute zone is dorso-frontal, and partially contralateral (Land and Eckert, 1985). In *H. tau* males, we recorded from both the forward, frontal acute zone and the dorsal one (Horridge, 1978), the latter characterized by photoreceptors tuned to shorter wavelengths of light (Laughlin and McGinness, 1978; Laughlin, 1976).

Visual stimuli

We presented and controlled visual stimuli at a 120 Hz frame rate using custom-written software implemented in MATLAB (MathWorks, Natick, MA, USA) and Psychtoolbox, with gamma calibration correction. For a given photoreceptor, we measured responses to moving bars of red, green and blue against a dark background to approximately classify spectral sensitivity and to locate the receptive field. We then investigated photoreceptor responses (signal-to-noise ratio, SNR) under light-adapted conditions (luminance on axis: 300 cd m^{-2}). To estimate target detectability thresholds, we drifted black square targets from left to right through the centre of the photoreceptor receptive field (for centre measure, see Rigosi et al., 2017). A minimum of 50 repetitions for each of 13 different target sizes (logarithmically spaced between 0.06 and 11 deg, corresponding to target areas from 0.004 to 121 deg^2, Weber contrast=−0.998) were randomly presented in the visual field of the same photoreceptor. For each species, we chose a target velocity below the threshold for acuity deterioration (40–70 deg s^{-1}), limiting blur to spatial rather than temporal processing (see, for example, Juusola and French, 1997; Snyder, 1977; van Hateren, 1993).

Analysis

Time domain

We measured the photoreceptor's receptive field at the beginning and end of each experimental set, allowing us to discard experiments where the receptive field location on the screen had drifted as a result of pathological disruption of the sharp electrode. The mean pre-stimulus response was subtracted to account for any drift in resting membrane potential. For a given target size, we removed noise from 'signal responses' by averaging 50–100 trials and low-pass filtering (third-order Butterworth filter, cut-off 70 Hz). The signal was then estimated as the amplitude of the average peak hyperpolarization induced by the dark targets. At the detection limits, this hyperpolarization is brief, because of the short time the dark target takes to transit through the receptive field. It is also small (<1 mV), as a result of the low effective contrast, as this blurred feature is imaged against the background, so successful detection would depend primarily on the noise distribution for the bright background of the white screen (300 cd m^{-2}). To estimate a reasonable noise threshold for detection, we therefore estimated the

standard deviation of the photoreceptor response to the white screen by calculating the difference between the standard deviation measured intracellularly (measurement noise+photoreceptor noise) and extracellularly (measurement noise) for each cell. To determine noise distributions, we concatenated trials in time (filtered with a third-order Butterworth filter, passband 0.5–200 Hz). For further details (Fig. 1A,B), see methods of Burton and Laughlin (2003) and Rigosi et al. (2017).

The SNR in the time domain (SNR$_T$), measured in decibels, was calculated as 10×log10(signal^2 noise^{-2}).

Frequency domain

We estimated the power spectrum of the signal response (averaged and filtered) for each target size (Fig. 1C). This was compared with the two noise spectra obtained from intracellular (blue line) and extracellular (green line) recordings to the white screen. Photoreceptor noise (red line) was determined as the difference between the two noise spectra (intracellular−extracellular). Matched with the temporal profile of the moving target, we calculated the band power over the frequency range 5–15 Hz by applying a Hamming window and using a periodogram power spectral density estimate for each signal response (varying target size) and the photoreceptor noise. The SNR in the frequency domain (SNR$_F$) was calculated as the ratio between the signal and photoreceptor noise band power measures within the 5–15 Hz range.

Estimated target size threshold and contrast sensitivity

In order to quantify the response threshold at the noise limits for each dataset (reported in Table 1), we first calculated the average slope of linear regression fits to our data (response as a function of target area) for targets small enough to confine evoked responses within the linear range (<2 mV). We then obtained their intersection with a 2× noise threshold. This value was used to estimate the effective contrast in the neural image for a target at this limit based on the photoreceptor acceptance angle (Δρ, Table 1) measured intracellularly in light-adapted eyes (see methods in Rigosi et al., 2017). An optical blur kernel based on this measured acceptance function was then convolved with the stimulus to estimate the target luminance distribution in the focal plane after optical blur, and thus the maximum effective luminance difference as such a feature passes the receptive field centre ('maximal neural contrast'; see O'Carroll and Wiederman, 2014).

RESULTS AND DISCUSSION

Photoreceptors detect black moving targets much smaller than their receptive field

In all four species, decreasing target area below ∼1 deg^2 resulted in a linear decrease in response amplitude (Fig. 2A, solid lines). This reflects the expected 'sub-pixel' resolution in effective target contrast (i.e. the decreased contrast in the blurred neural image; O'Carroll and Wiederman, 2014). For target sizes larger than the photoreceptor receptive field, responses saturate at around 15–20 mV below resting potential. The highest signal sensitivity was observed in dragonfly photoreceptors (*H. tau*), followed by the hoverfly (*E. tenax*), blowfly (*C. stygia*) and the honey bee drone (*A. mellifera*). Dashed lines in Fig. 2A show average photoreceptor noise (1× s.d.) for each species. This was lowest in blue-sensitive dragonfly photoreceptors and highest in the blowfly. Fig. 2B expresses data as the SNR, an engineering standard. A high SNR results from either high response sensitivity or low levels of noise. For example, the SNR of blue-sensitive dragonfly photoreceptors is
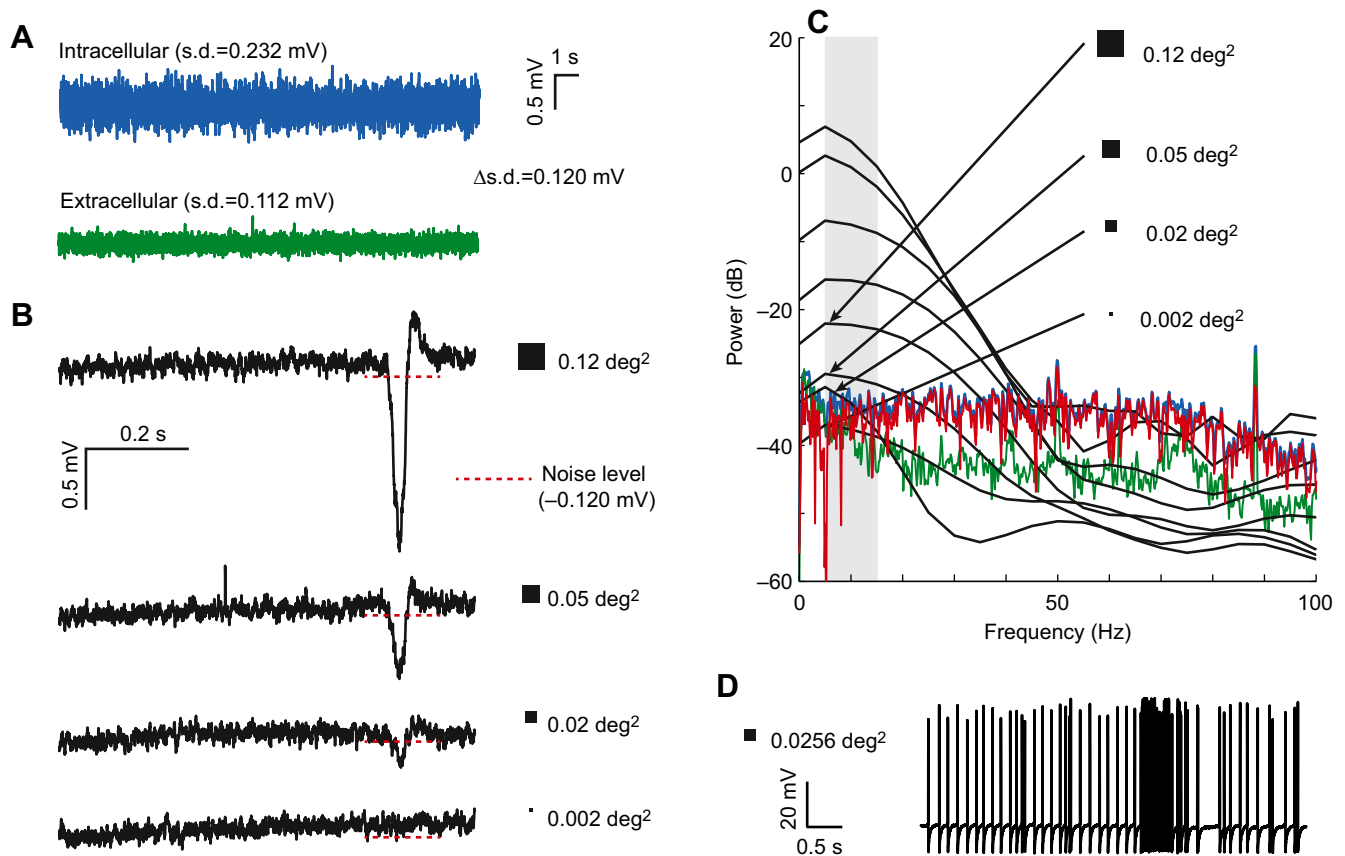
Fig. 1. Example of signal analysis in both time and frequency domains in a dorsal photoreceptor of a male hoverfly, *Eristalis tenax*.
(A) Photoreceptor noise (red dotted lines in B) was calculated as the difference between the s.d. of the intracellular response to a white screen stimulus for 20 s (blue line) and the response obtained to the same stimulus in the extracellular space (green line). (B) Averaged time response (*N*=50 per stimulus size) to a black target (four different angular sizes) in the same photoreceptor as in A. (C) Power spectra of the target responses in B and four larger targets (black lines), together with noise spectra presented in A. Grey area denotes the frequency range used in the measure of signal-to-noise ratio (SNR). (D) Neural response of a target-detecting neuron (CSTMD1) in *Hemicordulia tau* when a small (0.16 deg×0.16 deg) black target was crossing its receptive field hotspot.

matched to that of their green-sensitive counterparts because of the lower observed noise levels. To confirm our time domain analysis, we also computed a frequency domain version of the SNR (Fig. 2C), which estimates the signal and noise components in the bandwidth relevant to this target-detection task (i.e. for this target velocity).

To quantify the target-detection threshold for each species (Fig. 2D), we plotted response sensitivity and the photoreceptor noise (1× and 2× the s.d., thus capturing 68% and 95% of noise measurements, respectively). On the same graphs, we plotted the SNR_T, which intersects the abscissa (target area) at a SNR of 0 decibels (1:1 ratio of signal to noise).

The most sensitive photoreceptors, in the dorsal acute zone of *H. tau*, were capable of detecting a luminance change equivalent to

a passing target just 0.14 deg in width (0.02 deg², 2× s.d. noise). This is around 7–8 times smaller than the angular size of the recorded photoreceptor receptive field for *H. tau* (Laughlin, 1973; and see Table 1). Interestingly, when we calculated the corresponding contrast of the target at this threshold, taking in consideration the optical blur of the photoreceptors (O'Carroll and Wiederman, 2014), we found that the contrast sensitivity was similarly high across species (thresholds ranging between 0.014 and 0.08 Weber contrast, Table 1). The dorsal acute photoreceptors of *H. tau* showed the highest contrast sensitivity, permitting detection of only a 1.4% change in luminance.

Key variables permitting photoreceptors to achieve high contrast gain and detect very small targets (below the nominal

Table 1. Detectability limit found in photoreceptors matches the limit for small-target detection in higher-order neurons or behavioural performances

Species	Eye type	Horizontal Δρ (deg)	A (deg²)	Max. neural contrast (at 2× noise)	A/√N (deg²)	Previously measured (deg²)
E. tenax	NS	0.86±0.06	0.0381	0.0441	0.015 (*N*=6)	0.04 (E)[a]
C. stygia	NS	0.92±0.02	0.0807	0.0797	0.033 (*N*=6)	0.25 (B)[b]
H. tau (B)	App.	1.10±0.04	0.0195	0.0142	0.008 (*N*=6)	0.0256 (E)[c]
H. tau (G)	App.	1.14±0.08	0.0316	0.0213	0.013 (*N*=6)	0.0256 (E)[c]
A. mellifera	App.	1.5±0.14	0.1616	0.0604	0.057 (*N*=8)	0.1681 (B)[d]

NS, neural superposition eyes; App., apposition eyes; Δρ, acceptance angle (mean±s.e.m.), obtained electrophysiologically in the light-adapted state; *A*, measured photoreceptor area threshold at 2× noise; *A*/√*N*, theoretical lamina limit, where *N* is the number of photoreceptors conveying to the same lamina cartridge; E, electrophysiological studies; B, behavioural studies: [a]Nordström et al., 2006; [b]Boeddeker and Egelhaaf, 2003 (note that this study was not conducted in *C. stygia* but in a related Calliphoridae); [c]Joseph M. Fabian, personal communication (Fig. 1D), spectral tuning unknown; [d]Vallet and Coles, 1993.
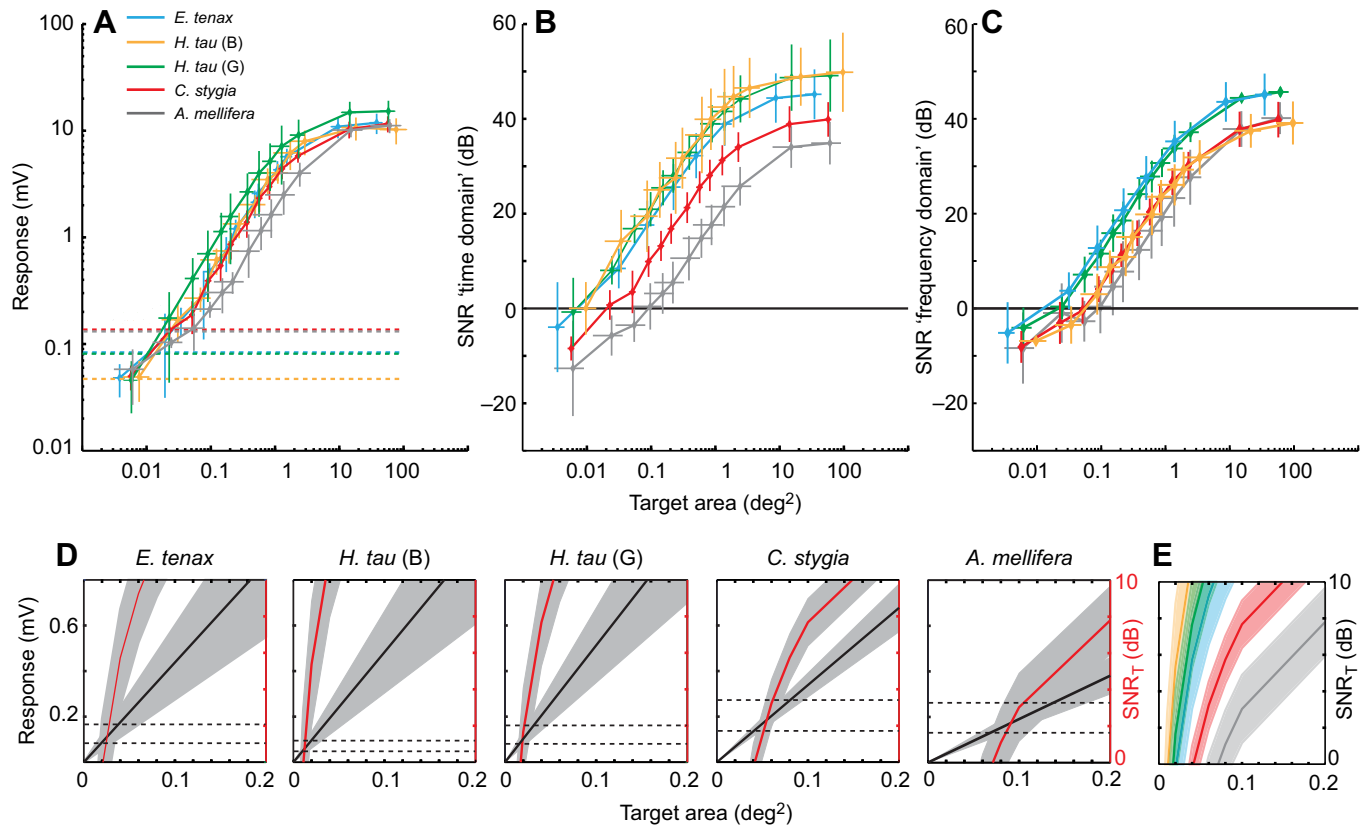
Fig. 2. Peak responses and SNR of small black moving targets in single photoreceptors of insect pursuers. (A) Mean±95% confidence interval (CI) peak responses to black moving targets of increasing area in the high-acuity area of male hoverflies (*Eristalis tenax*, *N*=7), dragonflies (*Hemicordulia tau*; B, blue photoreceptors, *N*=6; G, green photoreceptors, *N*=5), blowflies (*Calliphora stygia*, *N*=9) and honey bees (*Apis mellifera*, *N*=5). Coloured dotted lines represent 1× noise of the averaged photoreceptor noise for each species. (B,C) Averaged SNR±95% CI for increasing object sizes of the same data as in A. Single SNR were calculated using the variance of single cell noise over peak responses (B) and in the frequency domain (C). *Eristalis tenax N*=5, *H. tau* B *N*=4, *H. tau* G *N*=3, *C. stygia N*=8, *A. mellifera N*=5. (D) Enlarged view of A and B for object areas ≤0.2 deg²; black lines represent peak responses calculated by plotting linear regression coefficients of responses <1 deg and red lines represent the SNR for the same object sizes. Horizontal dotted lines represent 1× and 2× s.d. of the averaged photoreceptor noise, correspondingly. Means±95% CI are presented. (E) SNR as in D in the different species; colours as in A.

photoreceptor receptive field) include the optics of the system, the phototransduction process and the light adaptation state of the eye. Even at consistently high light levels (all species in this study are diurnal), insect compound eyes have evolved different strategies to optimize target detection. The most common is the 'acute zone', an eye region that provides higher resolution within a subset of the visual field – analogous to the fovea of the human eye. Acute zones have larger facet lenses that provide a sharper optical image via the reduced diameter of the Airy diffraction pattern. This is then sampled by correspondingly smaller diameter rhabdoms with smaller interommatidial angles to provide a higher angular 'pixel' density (Land and Eckert, 1985; Anderson and Laughlin, 2000; Horridge, 1978; Stavenga, 2003), as we probably observed in the dragonfly (Laughlin, 1973). An alternative solution is the so-called 'bright zone' eye, a sub-region where facet diameter is also enlarged, but where the associated sampling by the retina utilizes larger photoreceptors and a similar sampling density to other eye regions, apparently 'wasting' the potential resolution of larger facet lenses (van Hateren et al., 1989; Straw et al., 2006). The larger angular acceptance of such an eye region leads to lower resolution compared with an acute zone; however, increased photon catch provides a higher SNR and thus high contrast sensitivity (Straw et al., 2006). In both designs, photoreceptor noise remains the ultimate limiting factor, but this might be higher in acute zone eyes, as a result of the shorter time an object would transit

through the receptive field (with a consequent reduced change in photon catch) (Srinivasan and Bernard, 1975; Burton and Laughlin, 2003). This might be compensated for by increased numbers of phototransduction units (e.g. longer rhabdoms) and correspondingly faster phototransduction cascades (decreased time constant), albeit at higher cost (Howard et al., 1987).

Target detection threshold varies among species
The high target detectability found in dragonflies and hoverflies (Fig. 2D) results from increased contrast sensitivity (slope of the black line) compared with the blowfly and honey bee drones, as well as a decreased noise level (dashed black lines). Both contribute to the larger gain in SNR with target size (slope of the red line). These data support previous reports of higher sensitivity in light-adapted *H. tau* photoreceptors compared with *C. stygia* (Laughlin and Hardie, 1978). Fig. 2E shows this SNR comparison across the species. High SNR in both *E. tenax* and *H. tau* is well suited to these highly specialized pursuer species (Olberg et al., 2005; Horridge, 1978; Nordström et al., 2006).

Interestingly, among the two dipteran species, *C. stygia* revealed higher noise than *E. tenax*. Previous work described dark-adapted photoreceptors in the Calliphoridae with larger and longer quantum bump events compared with *E. tenax* (Laughlin and Weckström, 1993). The measured gain obtained in *C. stygia* (3.39± 0.8 mV deg⁻²) closely matches what we previously described

(3.4 mV deg^{-2}, O'Carroll and Wiederman, 2014), although this is an entirely new dataset.

Our data show that in honey bee drones, contrast gain is 2.5 times lower than in *H. tau*. This sensitivity (1.9±0.4 mV deg^{-2}) is, nevertheless, remarkably high compared with gain measured recently in the acute zone of honey bee foragers: 1.08± 0.2 mV deg^{-2} (Rigosi et al., 2017). This result reveals the functional effectiveness of the underlying morphological specializations (Menzel et al., 1991) that tune the male eye for pursuing a queen.

For the time domain analysis, the SNR (Fig. 2B) is simply the mathematical ratio of signal and noise values (Fig. 2A). Thus, the target response that intersects 1× s.d. of noise is mathematically equivalent to the 0 dB limit (equal to a 1:1 SNR). In contrast, our frequency domain SNR measure (Fig. 2C) restricts analysis to the range 5–15 Hz, providing a more specific measure for how the temporal profile of the target response is corrupted by the noise profile in the corresponding bandwidth. We included this analysis for validation and were surprised to note a single difference in the resultant curves (compare Fig. 2B with C). Photoreceptors of the dorsal area of *H. tau* shifted to the right, indicating worse performance (yellow line, Fig. 2B cf. C). Examining the individual spectra, we tracked this decrease in SNR$_F$ to higher noise levels within this passband (i.e. 5–15 Hz), rather than a reduction in signal strength. This was not observed in the time analysis and indicates differences in the distribution of noise across the frequency domain.

Target detection threshold in photoreceptors matches the small-target detection limit of the animal

The limit for 'sub-pixel' resolution of targets by photoreceptors closely matches the target detection limit previously found in these species (Table 1). Hoverfly STMD neurons (*E. tenax*) have been shown to respond to drifting black targets subtending an area of 0.04 deg^2 (Nordström et al., 2006), closely matching to our calculated photoreceptor threshold of 0.038 deg^2 (Table 1). CSTMD1, a well-studied STMD neuron in the dragonfly *H. tau*, responds to 0.0256 deg^2 targets drifted through the most sensitive region of the receptive field (e.g. Fig. 1D). This appears to be the lower limit of sensitivity of CSTMD1 (and other STMDs). There are no direct measures for target detection in *C. stygia* but behavioural data and simulations in males of related Calliphoridae showed tuning when pursuing small targets also below the angular size of single ommatidia (Boeddeker and Egelhaaf, 2003). Honey bee drones will chase a dummy queen as small as 0.41 deg (0.1681 deg^2) (Vallet and Coles, 1993), a value closely matched by our photoreceptor threshold of 0.1616 deg^2. This match importantly reveals the effectiveness of a potent motivational cue (i.e. mating) that faithfully reveals the physiological limit of feature detection in a behavioural paradigm, compared with our recent data for forager females, where the physiologically measured limit is well below anything reported behaviourally (Rigosi et al., 2017).

Considering that our results were obtained in single photoreceptors, these findings might underestimate the peripheral sensitivity for small targets. At the single lamina cartridge, where a number of photoreceptors (N) are pooled together, there might be an improvement in the SNR equal to $\sqrt{N}$ (Land, 1997). This theoretical enhanced sensitivity (equal to $\sqrt{6}$ in the case of Diptera) could be crucial in maintaining a high sensitivity when environmental factors decrease the photoreceptor gain, such as dim light or cluttered environments. Our results nevertheless indicate that target detectability is established at the periphery, leaving higher brain areas more exquisitely tuned in providing further sharpening of target detectability, for example, when contrast is lowered as a result of dimmer or cluttered environments or when the animal experiences high angular velocities. This frees up higher areas for performing tasks of target extraction and mediating visual pursuit (such as predictive coding and selective attention).

Author contributions
Conceptualization: E.R., S.D.W., D.C.O.; Methodology: S.D.W., D.C.O.; Software: S.D.W., D.C.O.; Validation: S.D.W., D.C.O.; Formal analysis: E.R., S.D.W., D.C.O.; Investigation: E.R.; Resources: S.D.W., D.C.O.; Data curation: E.R.; Writing - original draft: E.R.; Writing - review & editing: S.D.W., D.C.O.; Visualization: E.R.; Supervision: S.D.W., D.C.O.; Project administration: S.D.W., D.C.O.; Funding acquisition: S.D.W., D.C.O.

References
Anderson, J. C. and Laughlin, S. B. (2000). Photoreceptor performance and the co-ordination of achromatic and chromatic inputs in the fly visual system. *Vision Res.* **40**, 13-31.

Boeddeker, N. and Egelhaaf, M. (2003). Steering a virtual blowfly: simulation of visual pursuit. *Proc. Biol. Sci.* **270**, 1971-1978.

Burton, B. G. and Laughlin, S. B. (2003). Neural images of pursuit targets in the photoreceptor arrays of male and female houseflies *Musca domestica*. *J. Exp. Biol.* **206**, 3963-3977.

Collett, T. (1971). Visual neurones for tracking moving targets. *Nature* **232**, 127-130.

Hardie, R. G. (1985). Functional organization of the fly retina. In *Progress in Sensory Physiology*, Vol. 5 (ed. D. Ottoson), pp. 1-79. Berlin, Heidelberg, New York: Springer.

Horridge, G. A. (1978). The separation of visual axes in apposition compound eyes. *Philos. Trans. R. Soc. Lond. B. Biol. Sci.* **285**, 1-59.

Howard, J., Blakeslee, B. and Laughlin, S. B. (1987). The intracellular pupil mechanism and photoreceptor signal: noise ratios in the fly *Lucilia cuprina*. *Proc. R. Soc. B Biol. Sci.* **231**, 415-435.

Juusola, M. and French, A. S. (1997). Visual acuity for moving objects in first- and second-order neurons of the fly compound eye. *J. Neurophysiol.* **77**, 1487-1495.

Land, M. F. (1997). Visual acuity in insects. *Annu. Rev. Entomol.* **42**, 147-177.

Land, M. F. and Eckert, H. (1985). Maps of the acute zones of fly eyes. *J. Comp. Physiol. A* **156**, 525-538.

Laughlin, S. B. (1973). Neural integration in the first optic neuropile of dragonflies I. Signal amplification in dark-adapted second-order neurons. *J. Comp. Physiol. A* **84**, 335-355.

Laughlin, S. B. (1976). The sensitivities of dragonfly photoreceptors and the voltage gain of transduction. *J. Comp. Physiol. A* **111**, 221-247.

Laughlin, S. B. and Hardie, R. C. (1978). Common strategies for light adaptation in the peripheral visual systems of fly and dragonfly. *J. Comp. Physiol. A* **128**, 319-340.

Laughlin, S. B. and Lillywhite, P. G. (1982). Intrinsic noise in locust photoreceptors. *J. Physiol.* **332**, 25-45.

Laughlin, S. and McGinness, S. (1978). The structures of dorsal and ventral regions of a dragonfly retina. *Cell Tissue Res.* **188**, 427-447.

Laughlin, S. B. and Weckström, M. (1993). Fast and slow photoreceptors - a comparative study of the functional diversity of coding and conductances in the Diptera. *J. Comp. Physiol. A* **172**, 593-609.

Lillywhite, P. G. (1977). Single photon signals and transduction in an insect eye. *J. Comp. Physiol. A* **122**, 189-200.

Menzel, J. G., Wunderer, H. and Stavenga, D. G. (1991). Functional morphology of the divided compound eye of the honeybee drone (*Apis Mellifera*). *Tissue Cell* **23**, 525-535.

Nordström, K. and O'Carroll, D. C. (2009). Feature detection and the hypercomplex property in insects. *Trends Neurosci.* **32**, 383-391.

Nordström, K., Barnett, P. D. and O'Carroll, D. C. (2006). Insect detection of small targets moving in visual clutter. *PLoS Biol.* **4**, e54.

Nordström, K., Bolzon, D. M. and O'Carroll, D. C. (2011). Spatial facilitation by a high-performance dragonfly target-detecting neuron. *Biol. Lett.* **7**, 588-592.

Olberg, R. M., Worthington, A. H., Fox, J. L., Bessette, C. E. and Loosemore, M. P. (2005). Prey size selection and distance estimation in foraging adult dragonflies. *J. Comp. Physiol. A* **191**, 791-797.

O'Carroll, D. (1993). Feature-detecting neurons in dragonflies. *Nature* **362**, 541-543.

O'Carroll, D. C. and Wiederman, S. D. (2014). Contrast sensitivity and the detection of moving patterns and features. *Philos. Trans. R. Soc. Lond. B. Biol. Sci.* **369**, 20130043.

Rigosi, E., Wiederman, S. D. and O'Carroll, D. C. (2017). Visual acuity of the honey bee retina and the limits for feature detection. *Sci. Rep.* **7**, 45972.

Sanes, J. R. and Zipursky, S. L. (2010). Design principles of insect and vertebrate visual systems. *Neuron* **66**, 15-36.

Seidl, R. (1982). Die Sehfelder und Ommatidien Divergenzwinkel von Arbeiterin, Königin und Drohne der Honigbiene (*Apis mellifera*). *PhD thesis*, Technische Hochschule Darmstadt.

Snyder, A. W. (1977). Acuity of compound eyes: physical limitations and design. *J. Comp. Physiol. A* **116**, 161-182.

Somanathan, H., Borges, R. M., Warrant, E. J. and Kelber, A. (2017). Visual adaptations for mate detection in the male carpenter bee *Xylocopa tenuiscapa*. *PLoS ONE* **12**, e0168452.

Srinivasan, M. V. and Bernard, G. D. (1975). The effect of motion on visual acuity of the compound eye: a theoretical analysis. *Vision Res.* **15**, 515-525.

Stavenga, D. G. (2003). Angular and spectral sensitivity of fly photoreceptors. I. Integrated facet lens and rhabdomere optics. *J. Comp. Physiol. A.* **189**, 1-17.

Strausfeld, N. J. (1991). Structural organization of male-specific visual neurons in calliphorid optic lobes. *J. Comp. Physiol. A* **169**, 379-393.

Straw, A. D., Warrant, E. J. and O'Carroll, D. C. (2006). A "bright zone" in male hoverfly (*Eristalis tenax*) eyes and associated faster motion detection and increased contrast sensitivity. *J. Exp. Biol.* **209**, 4339-4354.

Trischler, C., Boeddeker, N. and Egelhaaf, M. (2007). Characterisation of a blowfly male-specific neuron using behaviourally generated visual stimuli. *J. Comp. Physiol. A* **193**, 559-572.

Vallet, A. M. and Coles, J. A. (1993). The perception of small objects by the drone honeybee. *J. Comp. Physiol. A* **172**, 183-188.

van Hateren, J. H. (1993). Three modes of spatiotemporal preprocessing by eyes. *J. Comp. Physiol. A* **172**, 583-591.

van Hateren, J. H., Rudolph, R. C. H. A., Laughlin, S. B. and Stavenga, D. G. (1989). The bright zone, a specialized dorsal eye region in the male blowfly *Chrysomyia megacephala*. *J. Comp. Physiol. A* **164**, 297-308.

Wardill, T. J., Knowles, K., Barlow, L., Tapia, G., Nordström, K., Olberg, R. M. and Gonzalez-Bellido, P. T. (2015). The killer fly hunger games: target size and speed predict decision to pursuit. *Brain. Behav. Evol.* **86**, 28-37.

Wiederman, S. D., Fabian, J. M., Dunbier, J. R. and O'Carroll, D. C. (2017). A predictive focus of gain modulation encodes target trajectories in insect vision. *Elife* **6**, e26478.